Numerical Analysis and Computational Modelling for Polymer-Based Biodegradable Contraceptive Implants

Westminster School John Locke Project

Senkai Hsia[a,b]

Principal Investigator: Professor W. Mark Saltzman, PhD[a]

Advisors: Gina Buzzelli[a] and Fan Yang[a]

[a] Saltzman Laboratory, Department of Biomedical Engineering, Yale University

55 Prospect Street, Malone Engineering Center, New Haven, CT 06520-8260, United States of America

[b] Departments of Physics and Mathematics, Westminster School

Little Dean's Yard, Great Smith St, RHSC 102, Westminster, London SW1P 3PF, United Kingdom

August 2018

1 Abstract

Current commercial contraceptive implants, while safe and effective, require invasive surgery to explant depleted rods. Polymer-based biodegradable contraceptive implants would eliminate this burden. We have recently investigated levonorgestrel (LNG) loaded Poly(ω–pentadecalactone-co-p-dioxanone) [poly(PDL-co-DO)] polymers for suitability for subcutaneous biodegradable contraceptive implants. 50mg implants composed of 28% LNG loaded poly(PDL-co-DO) were assessed for release *in vitro* and *in vivo* in rats. Here, we use numerical analysis techniques to evaluate the relationship (IVIVC) between collected *in vivo* and *in vitro* implant studies. We then employ computational modelling methods to simulate *in vivo* performance based on *in vitro* data input. A strong Level A IVIVC linear correlation ($R^2 = 0.995$) was achieved between *in vivo* and *in vitro* data, and validation methods yielded a prediction error to a fitted model of observed data of 7.6%. Computational modelling of drug release based on *in vitro* data yielded predicted *in vivo* profiles of similar shape and order of magnitude to observed data. Our results demonstrate the reliability of *in vitro* studies to accurately simulate biological conditions, and progress computational models to predict drug release behaviour, informing future engineering directions to optimise implant efficacy.

Contents

2 Introduction

2.1 Biodegradable Contraceptive Implants

Subcutaneous implants are relied upon across the world as a safe and highly effective form of contraceptive for women. Such contraceptives utilise levonorgestrel (LNG) as the active drug, which is released into the surrounding tissue and bloodstream at a predictable and consistent rate over several years. After 30 years since their introduction, implants continue to be a popular choice due to their long-term protection, low maintenance and tolerable side effects [1].

However, subcutaneous implants pose a number of challenges to recipients. Commercial examples such as Jadelle®(Bayer AG, Leverkusen, Germany) are often made of non-biodegradable materials such as silicon. As a result, after completion of drug release, invasive surgery is required to ex-plant the depleted rods. This poses a particular difficulty in developing nations: where the pre-requisite surgical expertise has much lower prevalence, medical infrastructure is less advanced, and as a result, there is a higher risk of post-operative complication [2]. Given that there continues to be a substantial demand for effective family planning and contraception in these communities, where most can ill-afford the surgery required under the *status quo*, fully biodegradable contraceptive implants would be a highly desirable solution to this problem.

2.2 Poly(ω–pentadecalactone-co-p-dioxanone) [poly(PDL-co-DO)]

Poly(ω–pentadecalactone-co-p-dioxanone) [poly(PDL-co-DO)] is a group of polyester copolymers that degrade upon contact with water by hydrolysis over time periods suitable to deliver long term contraception [3]. Previous publications have demonstrated that this polymer demonstrates properties that are desirable for this purpose, such as being stable when inserted subcutaneously and an ability to be formulated into particles to slowly release siRNA and chemotherapy drugs [4]. Importantly, poly(PDL-co-DO)'s semicrystalline structure across a range of copolymer formulations enables it to be optimally engineered with a varying degradation and drug release rates to suit specific biomedical contexts. Through subsequent work conducted by W. Mark Saltzman's research group at Yale University, we have shown that poly(PDL-co-DO) can be engineered into a biodegradable contraceptive

implant to release LNG at a constant rate for over 12 months [5]. Here, by performing numerical analysis of our collected experimental data collected in laboratory and animal studies, and using computational methods, we demonstrate mathematical relationships and predictability in our results to aid future polymer based degradable contraceptive engineering.

2.3 *In Vivo – In Vitro* Correlation (IVIVC)

In vitro – in vivo correlation (IVIVC) is defined by the United States Food and Drug Administration (FDA) as a predictive mathematical model describing the relationship between an *in vitro* property and a relevant *in vivo* response of drug products [6]. *In vitro* data collected from drug products resting in solution is commonly presented as a cumulative release profile over time, whereas *in vivo* data taken from animal studies is shown as a profile of concentration of drug released into the blood plasma. While experimental collection and data presentation methods differ, given that the same amount and chemical composition of drug is undergoing release in both cases, a quantifiable relationship should exist between these two data sets.

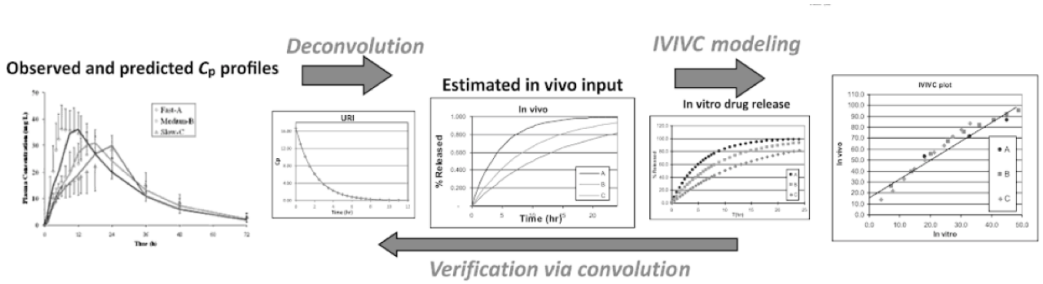

Figure 1: Diagram illustrating the process of developing an IVIVC. This is described in greater detail in Methods [7].

Such an IVIVC mathematical relationship is crucial to engineers and pharmaceutical scientists in drug development. Firstly, they are essential to validating experimental data from laboratory studies when applied to subsequent animal studies. The ability to show a correlation between *in vivo* and *in vitro* results demonstrates that *in vivo* parameters were correctly modelled in the *in vitro* study and are therefore reliable [7]. Secondly, IVIVC is most often used to obtain bio-wavers from the FDA to bypass or reduce the number of human clinical trials [6]. These are often the most cost intensive phase of

drug development and present the most risk to pharmaceutical development, and such a bio-waver allows for drugs to enter the market more cost effectively and efficiently. Finally, from an engineering standpoint, such a correlation enables the creation and validation of mathematical models used to simulate drug release *in vivo* and *in vitro*, and therefore to inform future drug design and engineering decisions to optimise performance.

2.4 Mathematical Models and Computational Predictions

The chemical processes involved in drug release and delivery have been well known and studied by bioengineers over recent decades, and mathematical models have been developed to describe the behaviour of these systems [8]. Assuming that drug release occurs by diffusion in a one compartment model (See Fig. 2), that is there is only one biological system of interaction in the release mechanism, there are two factors whose parameters must be calculated to accurately model *in vivo* drug release behaviour. The first is the constant of absorption, K_a, which describes the linear rate which a drug is initially diffuses out into the bloodstream from its initial concentration. The second is the constant of elimination, K_{el}, which describes the linear rate which drug is cleared from the biological system through metabolic and waste processes. These two constants are used to exponentially model the decay in concentration of drug over time, and therefore describe the burst phase and elimination phase as shown in Fig. 3 [9].

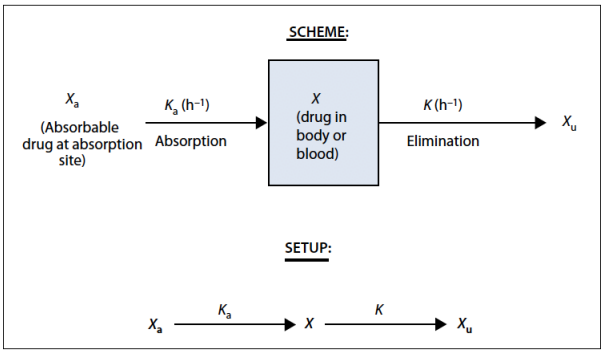

Figure 2: Diagram for a one compartment model where X_a is the mass of drug at the site of administration,; X_u is the mass or amount of drug excreted unchanged in the urine at time t, K_a is the first-order absorption rate constant(h^{-1}); and K is the first-order elimination rate constant (h^{-1}) [9].

Prediction of drug release by computational modelling is useful for validation, engineering and cost efficacy as previously described. Prediction of *in vitro* cumulative release profile requires employment of partial differential equation (PDE) models [10], which are beyond the scope of this paper. However, it is possible to predict *in vivo* release profiles based on an *in vitro* input profile without resorting to PDEs [11]. In our case, such a procedure would result in a reduced need for expensive animal studies and much faster improvement time-scale to optimise implant efficacy. Here, we demonstrate that computational methods can successfully predict *in vivo* concentration profiles and validate experimental results.

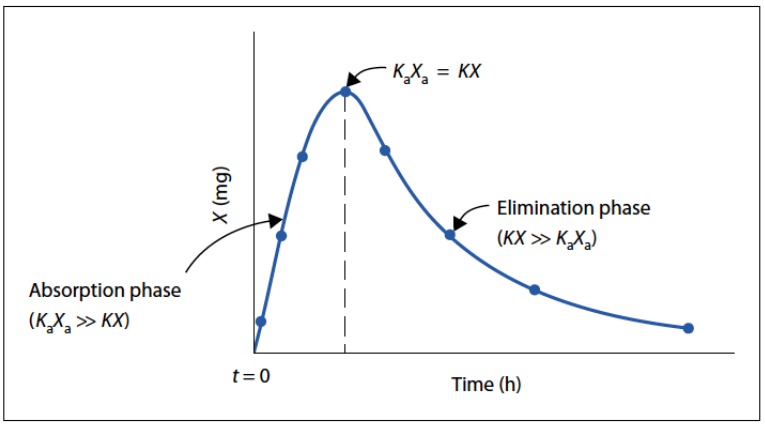

Figure 3: Graph showing a typical *in vivo* drug blood plasma concentration profile over time. This profile is modelled as a function over time by the Bateman multi-exponential decay equation, a modified form of which is shown as Equation 1, used for curve fitting in IVIVC Methods. [9]

3 Materials and Methods

3.1 Polymer Synthesis, Implant Manufacture and Study Set-up

Poly(PDL-co-DO) was produced according to ring-open copolymerisation between ω–pentadecalactone (PDL) and p-dioxanone (DO), as shown in Fig 4 [4, 5].

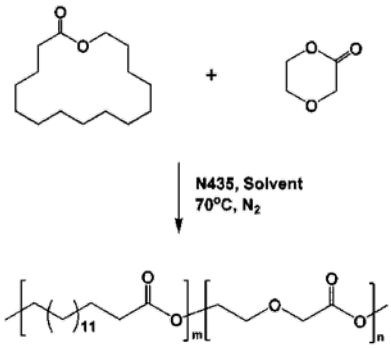

Figure 4: Ring-opening copolymerization between PDL and DO to make poly(PDL-co-DO)

Implants were then manufactured according to a variety of methods described in previous publications [5]. Generally, assayed volumes of LNG were added to dichloromethane (Sigma-Aldrich, St Louis, Missouri, United States) to form a solution. The solution was then vaporised or evaporated to form an LNG and polymer mixture. This mixture was then placed into a proprietary mold and was compressed to produce solid implants of approximately 50mg by weight and 1cm by length.

LNG loaded Poly(PDL-co-DO) implants were incubated 1 mL of phosphate buffered saline (PBS) solution (pH=7.4) containing 3% methyl-beta-cyclodextrin (M-β-CD) at 37^{o}C. At selected time points, the buffer solution, in which the implant had been continuously resting and fully submerged, was collected and replaced. The collected solutions were analysed for LNG by high-performance liquid chromatography (HPLC) for LNG content as described below.

LNG loaded Poly (PDL-co-DO) implants were also implanted subcutaneously into 9 live rat specimens. At selected time points, blood samples were collected and analysed for blood plasma concentration as described below.

3.2 Data Collection

As described in previous publications [5], for *in vitro* HPLC, a Waters C18 column (WAT086684) was used for LNG quantitation. Solvent A was 0.1% Trifluoroacetic Acid (TFA) in HPLC grade water, and solvent B was 0.1% TFA in HPLC grade acetonitrile. Initial solvent B concentration was set at 5% and allowed to increase to 90% by the 20th minute. Flow was maintained for 5 min at this level before dropping to 5% at the 27th minute, which was maintained until the end of the run at 30 minutes. LNG was detected at a wavelength of 240nm. Oven temperature was 30^{o}C, and 45μl of solution was injected for each sample run. Meanwhile, *in vivo* blood samples were sent to a commercial column chromatography analysis company to obtain an LNG plasma concentration profile in a manner analogous to the HPLC.

3.3 IVIVC

In vivo LNG blood plasma concentration results and *in vitro* cumulative LNG dissolution data were collected over periods of 581 and 297 days respectively with 50mg by weight and 28% LNG-loaded poly (PDL-co-DO) (Mw = 100K) implants. Using *in vitro* data from 50mg by weight and 28% LNG-loaded poly (PDL-co-DO) (Mw = 50K) implants, and after adjusting with a scale factor to account for increased LNG mass, estimated *in vitro* data for the 50mg by weight (Mw = 50K) polymer was extrapolated to 714 days.

In both data sets, outliers were identified and ignored according to the Tukey's Fences method (IQR rule) where k equals 1.5. To perform a Level A IVIVC analysis, *in vivo* data for all 9 samples were fitted to a single curve using the Curve Fitting Application in MATLAB (MATLAB and Curve Fitting Toolbox Release 2017b, The MathWorks, Inc., Natick, Massachusetts, United States) according to the following multi-exponential equation [11]:

$$C_p(t) = a(e^{-K_{el}t} - e^{-K_a t}) + b \tag{1}$$

where $C_p(t)$ is the concentration of LNG in the blood plasma at time t, K_a is the absorption rate constant, K_{el} the elimination rate constant, a is a constant representing the intercept of the concentration-time plot, and b represents a constant fitted in MATLAB to optimize the fitting of the graph.

The Curve Fitting tool utilizes non-linear least squares regression analysis to best fit the observed data to the equation. The coefficients derived were then used as the values for K_{el} and K_a.

The Wagner-Nelson deconvolution method was then applied using MATLAB, assuming a one compartment model, to obtain the fraction of LNG absorbed from the *in vivo* plasma concentration curve. The following equation was used for each assayed time point [11]:

$$C_a(t) = \frac{C_p(t) + K_{el} \int_0^t C_p(t)dt}{K_{el} \int_0^{t_{\max}} C_p(t)dt} \tag{2}$$

where $C_a(t)$ is the fraction of LNG absorbed at time t, $C_p(t)$ is the concentration of LNG in the blood plasma at time t, and $t_{\max}$ is the theoretical time when all the drug has been released. LNG percentage released *in vitro* were calculated from the cumulative dissolution curves for all 4 samples and averaged.

A Levy plot was also used to compare time points in the *in vivo* and *in vitro* data that absorbed or released similar percentages of LNG respectively [7]. Time points with differences of less than or equal to 0.5% were selected and plotted. A linear regression line was then fitted and a Pearson correlation coefficient and a coefficient of determination (R^2) were calculated.

3.4 Validation

Predicted *in vivo* percentage absorbed values were obtained for each *in vitro* assayed time point using the linear regression IVIVC line fitted by MATLAB. The predicted *in vivo* absorbed values were then convoluted to give blood plasma concentrations using the following iterative equation derived from the Wagner-Nelson method [12]:

$$C_p(t+1) = \frac{(2 * \Delta F * D) + C_p(t)(2 - K_{el} * \Delta t)}{(2 + K_{el} * \Delta t)} \tag{3}$$

where: $\Delta F = C_P(t+1) - C_p(t)$

And Δt equals the difference between two consecutive assayed time points *(t +1)* and *(t)*.

The resulting predicted LNG blood plasma concentration curve was then compared against the fitted multi-exponential curve obtained in 3.2 and a percentage error was calculated for each time point and averaged.

3.5 Computational Modelling

3.5.1 *In Vivo* Prediction by Superposition

In vitro cumulative dissolution data for all 4 samples was averaged and converted to give the average mass of LNG released per day between each assayed time point. The following formula was then applied iteratively to each mass of drug released over time [13]:

$$M(t+1) = M(t)e^{-K_{el}(\Delta t)} \tag{4}$$

where Δt equals the difference between two consecutive assayed time points *(t +1)* and *(t),* and M is the mass of LNG at time t.

The total mass of drug estimated to be in the *in vivo* system for any time was calculated by adding the mass of LNG released daily over any time period with the remaining mass of drug from previous time points remaining according to the equation, in a similar manner to superposition. The predicted blood plasma concentration was thereby calculated according to the following equation [13]:

$$C_p(t) = \frac{M(t)B}{V_d W} \tag{5}$$

where B is the bioavailability of LNG (assumed to be 1), V_d is the apparent volume of distribution of LNG, and W is the body weight (in the case of an arbitrary rat, estimated to be at 500g). The resulting plasma concentration release curve was then compared with the observed *in vivo* release and the fitted concentration model.

3.5.2 *In Vivo* Prediction by Numerical Convolution

Given that the dynamics of the system are assumed to be linear, linear systems theory enables *in vitro* dissolution-time profiles to computationally predict *in vivo* response. To do this, the *in vivo* and *in vitro* profiles must be converted from the time domain to the frequency domain. This enables

multiplication and division to act as convolution and deconvolution respectively. A transfer function relating an input function to its causal output can be created in the frequency domain as the ratio of the output function to its corresponding input function. This transfer function must be created from a reference dosage form to enable prediction of *in vivo* plasma concentration for other formulations [14]. *In vivo* and *in vitro* data from the 50mg by weight and 28% LNG-loaded poly(PDL-co-DO) implants was selected as the reference formulation to create the transfer function. To convert any function from time space to frequency space, its Laplace Transform must be taken, as defined by:

$$F(s) = \int_0^\infty f(t)e^{-st}dt \tag{6}$$

Given its many similar properties, for the purposes of data analysis the Fourier transform of a function over time was used as the equivalent of its Laplace transform as demonstrated by [15]:

$$\begin{aligned}\hat{f}(\omega) &= \mathcal{F}\{f(t)\} \\ &= \mathcal{L}\{f(t)\}|_{s=i\omega} = F(s)|_{s=i\omega} \\ &= \int_{-\infty}^{\infty} e^{-i\omega t} f(t)\, dt\ .\end{aligned}$$

First the *in vitro* cumulative dissolution profile for the 28% LNG-loaded poly(PDL-co-DO) loading was fitted in MATLAB's Curve Fitting Toolbox to a multi exponential equation of the form:

$$y = a * e^{bx} + c * e^{dx} \tag{7}$$

Fourier transforms were then taken of the fitted *in vivo* and *in vitro* profiles using MATLAB's "Fast Fourier Transform" function. The transfer function was then calculated by the following equation in frequency space [14]:

$$T(\omega) = \frac{C_p(\omega)_r}{D(\omega)_r} \tag{8}$$

where ω is the frequency in Hertz, T(ω) is the transfer function, $C_p(\omega)_r$ is the Fourier transform of the fitted reference *in vivo* LNG blood plasma concentration profile, and $D(\omega)_r$ is the Fourier transform of the fitted cumulative reference *in vitro* dissolution profile.

In vitro data from 50mg by weight and 27% LNG-loaded poly (PDL-co-DO) implants was selected and fitted according to the same exponential model as equation 8. The Fourier transform was then applied to the resulting equation. To yield the predicted *in vivo* response profile in frequency space, the *in vitro* Fourier transform was then multiplied by the transfer function in frequency space and by a scale factor X. This scale factor was used to adjust the magnitude of the transfer function to account for the difference in the actual amount of drug in the system compared with the reference formulation. This process is summarized by the following equation [14]:

$$C_p(\omega)_{\text{Pred}} = \frac{C_p(\omega)_r}{D(\omega)_r} D(\omega)_n X \tag{9}$$

where $C_p(\omega)_{\text{Pred}}$ is the predicted *in vivo* LNG plasma concentration in frequency space, and $D(\omega)_n$ is the Fourier transform of the fitted cumulative *in vitro* dissolution profile for an nth formulation. Finally, the inverse Fourier transform was applied to the resulting function in MATLAB to yield the predicted plasma concentration profile in the time domain. The above process is summarised in appendix Figure B.

Sections 3.3-3.5.2 are summarised in appendix Figure A.

4 Results and Discussion

4.1 *In Vivo* Daily Release

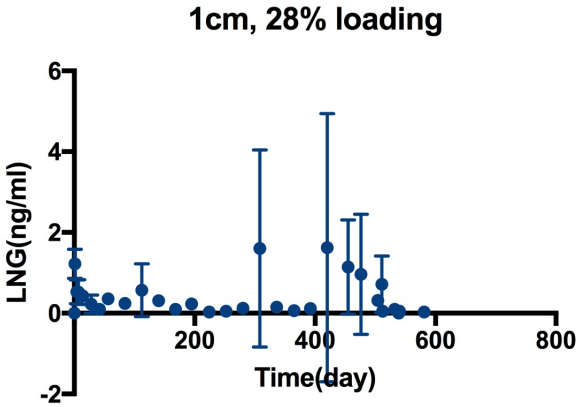

Figure 5: Mean LNG concentration in the blood plasma plotted over time.

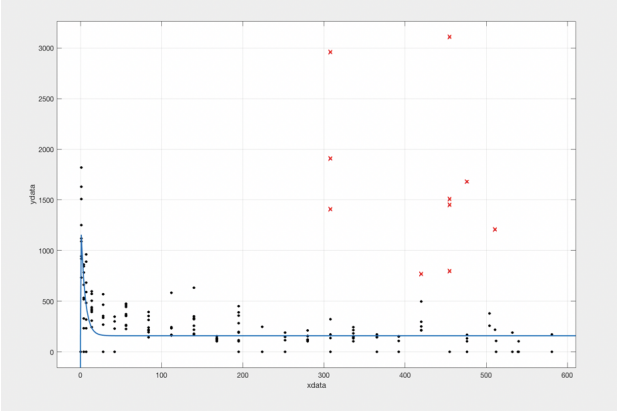

Figure 6: Curve fitting of *in vivo* plasma concentration profile within MATLAB.

Results from the *in vivo* study broadly fit the exponential decay release profile expected from *in vivo* release as shown in Fig. 3. However, there was significant variation and multiple anomalies in the data. Outliers existed well outside 2 standard deviations of the values collected at that time point. Additonal anomalies were largely values where "negligible" concentration was measured, but where LNG concentrations were clearly defined in the immediately preceding and following time points. Therefore, given the random nature of variation in error, we believe that these anomalies were more likely due a combination of natural biological factors and inaccuracies caused by the independent

commercial analysis, rather than a fault of experimental procedure. Statistical methods were then employed to identify and eliminate outliers according to the Tukey Fences method. This resulted in a smoother profile that could result in a more accurate curve fitting in MATLAB, which resulted in an improvement of R^2 coefficient of determination from 0.2 to 0.62.

We proceeded with the deconvolution using this fit because, in the absence of a reason to alter the biological system assumptions, it would be inappropriate to create a higher order model for the sake of a better fit. The Bateman equation used in this case therefore was the simplest model to describe a one-compartment model by exponential decay which fit the data to a reasonable degree of accuracy [9]. Additionally, the "fudge term" added onto the equation to optimise the fit may have been due to a mass equivalence condition occurring as LNG was absorbed into the surrounding tissue and then into the bloodstream.

4.2 *In Vitro* Cumulative Release

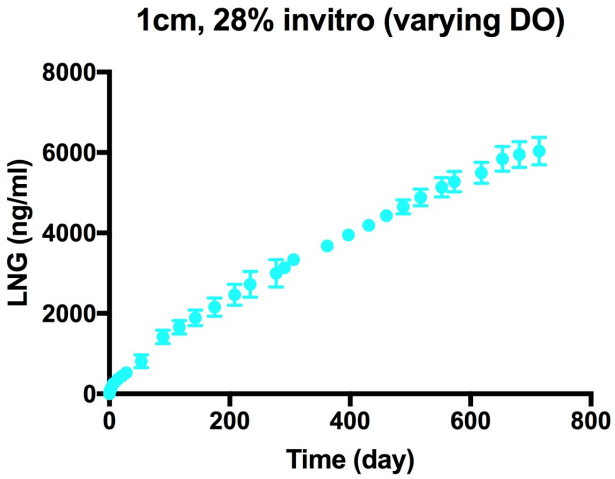

Figure 7: Mean mass of LNG released cumulatively plotted over time.

After extrapolation using the (Mw=50K) data to 714 days, the resulting cumulative release profile was smooth and as anticipated, with no significant anomalies or outliers. Therefore, the multi-exponential model described by Equation 7 fitted extremely well with the data, with an R^2 coefficient of determination of 0.999.

4.3 IVIVC

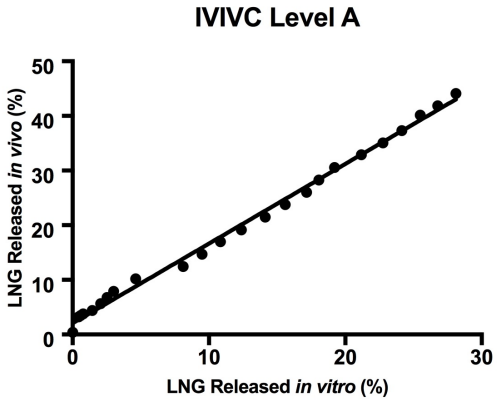

Figure 8: The percentage of LNG released *in vivo* over the percentage of LNG released *in vitro* was plotted and a linear regression line was fitted. The coefficient of determination, $R^2 = 0.995$ and the Pearson correlation coefficient = 0.998.

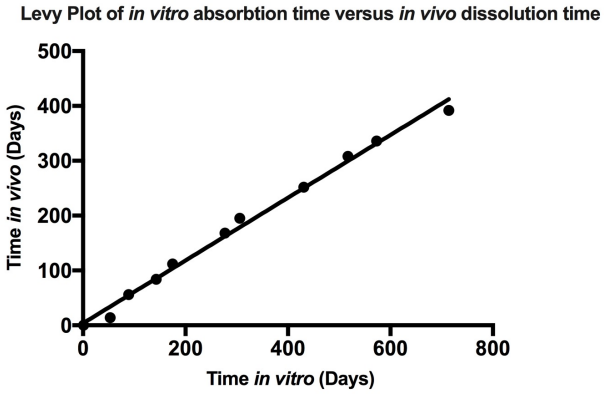

Figure 9: Equivalent time points of *in vivo* and *in vitro* percentage release were plotted as described in method 2 and a linear regression line was fitted. The coefficient of determination, $R^2 = 0.992$ and the Pearson correlation coefficient = 0.996.

After performing deconvolution, a very strong linear correlation was achieved between LNG released *in vitro* and LNG released *in vivo* as shown in Fig. 8. This suggests that a mathematical relationship exists between the two data sets and therefore the *in vitro* study accurately release accounted for biological conditions. Only 24 data points were plotted due to anomalies in the data set preventing a complete integration in the Wagner-Nelson method up to the assayed 35 time points.

The Levy plot, Fig. 9, demonstrates a very strong linear correlation between time points of equivalent release percentage. This suggests a strong linear time scaling between release rates between *in vivo* and *in vitro* and that the *in vitro* profile and *in vivo* profiles are mathematically similar. This therefore suggests that both studies exhibit similar release properties.

4.4 Validation

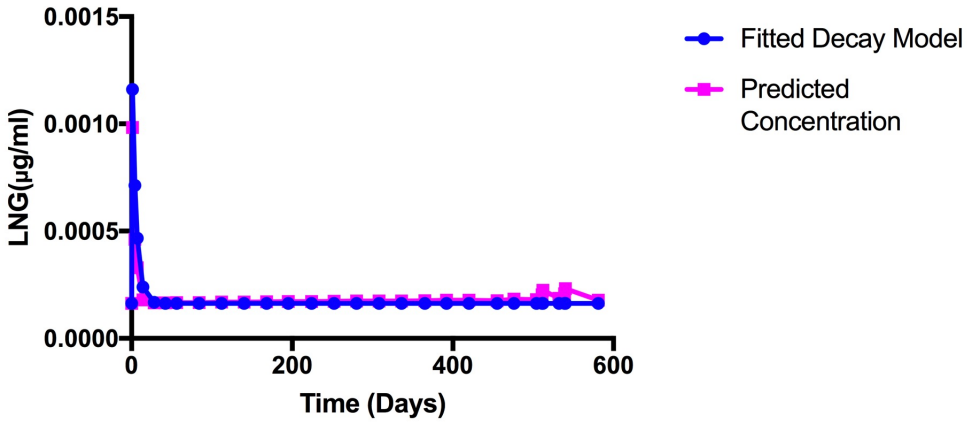

Figure 10: The predicted plasma concentration yielded from the IVIVC was plotted over time on the same axis as the fitted concentration model. The average percentage error to the fitted concentration model was 7.6%.

The results from the predicted plasma concentration suggests that the IVIVC is accurate, with an average prediction error of under 10%. This falls within FDA guidelines to verify a Level A IVIVC (that is a point to point percentage released correlation) which represents the highest level of correlation and is the most useful for obtaining biowavers.

4.5 Computational Modelling

4.5.1 *In Vivo* Prediction by Superposition

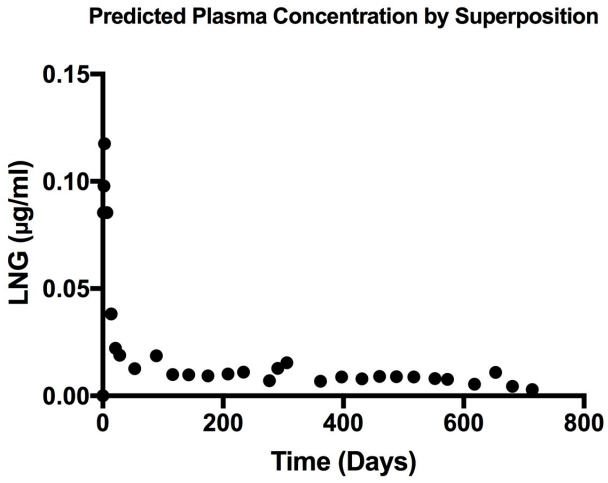

Figure 11: Predicted *in vivo* plasma concentrations of LNG yielded from the superposition method were plotted over time.

The results of the *in vivo* prediction by superposition were mixed. While the shape of the resulting function mapped a similar profile to the observed values, there was several orders of magnitude of discrepancy in LNG concentration. This may have been due to the model not accounting for the absorption rate constant due to there being no intermediary time values in the first initial day of release to account for this behaviour, and therefore the resultant profile yielded higher concentration results.

4.5.2 *In Vivo* Prediction by Numerical Convolution

The predicted *in vivo* plasma concentration profile yielded from the numerical convolution method with the 27 % LNG loaded polymer demonstrated more promising results. As shown in Fig. 12, the profile shape matched the observed concentration profile for the 28% LNG loaded polymer, and was on the same order of magnitude. A percentage error to validate this would be inappropriate in this instance, as the comparison would be between two different drug loadings. However, as the closest formulation to the observed *in vitro* data, there was less than a 0.0001 ($\mu g/ml$) difference in values

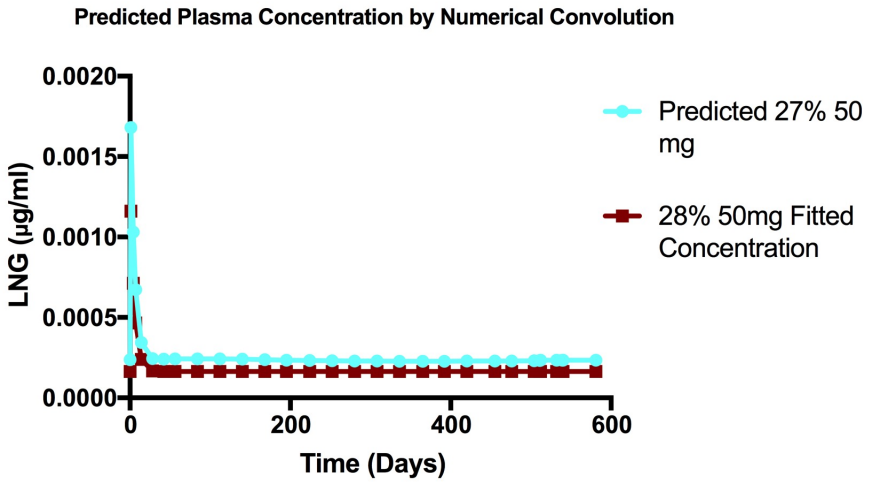

Figure 12: Predicted *in vivo* plasma concentration yielded from numerical convolution was plotted over time on the same axis as the fitted concentration model. The predicted concentration matched the same shape and was on the same order of magnitude as the fitted model.

for 29 out of the 30 data points. This suggests that this method yields an accurate prediction and can therefore be used to predict *in vivo* performance for a range of other formulations.

5 Conclusion

Through numerical analysis, we have demonstrated that there is a strong IVIVC between experimental studies conducted in the laboratory and in animal studies. Therefore, *in vitro* studies are now verifiable and there is a reduced need for animal trials. By developing and employing computational methods, we have successfully predicted *in vivo* release profiles from input *in vitro* data. Therefore, numerical prediction and optimisation of performance through design and computational simulation is now possible. Future investigation using PDEs to model behaviour independent of collected data remains to be done. Additionally, large scale manufacture processes and clinical trials are future hurdles to be overcome for biodegradable contraceptive implant development. Importantly, the application of these initial computational and mathematical methods will help engineer progress towards reducing and eliminating the need for costly invasive surgery to explant subcutaneous contraceptives. We hope this will one day improve recipient outcomes across the world and better their quality of life.

6 Acknowledgements

This research was supported through funding from the Bill and Melinda Gates Foundation, supervised through FHI 360, The United States Agency for International Development (USAID) and, indirectly, by the Goizueta Foundation and Yale University.

The author wishes to express special thanks to Professor Saltzman for his guidance, constructive feedback and for providing the unique opportunity to work on this research project. Thank you to Gina Buzzelli and Fan Yang for being my guardian angels, coming to my aid in overcoming challenges every day (of which there were many!) and above all, for their kindness and patience. Finally, many thanks to Alex Josowitz, Hanna Mandl, Amy Kauffman, PhD and the Saltzman Research Group at Yale Bioengineering for their kind welcome, support and for many, many laughs.

7 References

[1] Donna Shoupe. *The Handbook of Contraception: A Guide for Practical Management (2 ed.)*. Humana Press, 2015.

[2] Central Intelligence Agency. *The World Factbook 2018*. Central Intelligence Agency, 2018.

[3] Z Jiang, Azim. H, RA Gross, ML Focarete, and M. Scandola. Lipase-catalyzed copolymerization of omega-pentadecalactone with p-dioxanone and characterization of copolymer thermal and crystalline properties. *Biomacromolecules*, 2007.

[4] Zhang SM Liu C Gross RA Kyriakides TR Liu J, Jiang Z and Saltzman WM. Biodegradation, biocompatibility, and drug delivery in poly(omega-pentadecalactone-co-p-dioxanone) copolyesters. *Biomaterials*, 2011.

[5] Fan Yang, Anthony Bianchi, Elias Quijano, Gina Buzzelli, Zhaozong Jiang, and Mark W. Saltzman. Biodegradable contraceptive implant made with poly(omega-pentadecalactone-co-p-dioxanone) [poly(pdl-co-do)] and levonorgestrel (lng). *for publication in Journal of Controlled Release*, 2018.

[6] Center for Drug Evaluation and Research (CDER). Guidance for industry, extended release oral dosage forms: Development, evaluation, and application of in vitro/in vivo correlations. Technical report, Food and Drug Administration, U.S. Department of Health and Human Services, 1997.

[7] Jie Shen and Diane J. Burgess. In vitro-in vivo correlation for complex non-oral drug products: Where do we stand? *Journal of Controlled Release*, 219:644 – 651, 2015. Drug Delivery Research in North America â Part I.

[8] W. Mark Saltzman. *Drug Delivery: Engineering Principles for Drug Therapy.* Oxford University Press, 2001.

[9] *Jambhekar, Sunil S; Breen, Philip J, 2nd Edition*, chapter 7. Pharmaceutical Press, 2012.

[10] Niloofar Alipourasiabi. Modeling of controlled drug delivery from a chitosan microparticle. Master's thesis, University of Toledo August, 2016.

[11] Laura Amann, Michael Gandal, Robert Lin, Yuling Liang, and Steven Siegel. In vitro in vivo correlations of scalable plga-risperidone implants for the treatment of schizophrenia. 27:1730–7, 08 2010.

[12] Mukesh Gohel, R R. Delvadia, Dhaivat Parikh, Mehul Zinzuwadia, Chirag Soni, K G Sarvaiya, Neelima R. Mehta, B R. Joshi, and A S. Dabhi. Simplified mathematical approach for back calculation in wagner-nelson method. 01 2005.

[13] Saeed A. Qureshi. In vitro-in vivo correlation (ivivc) and determining drug concentrations in blood from dissolution testing – a simple and practical approach. *The Open Drug Delivery Journal*, 2014.

[14] Victor F. Smolen and Randall J. Erb. Predictive conversion of in vitro drug dissolution data into in vivo drug response versus time profiles exemplified for plasma levels of warfarin. *Journal of Pharmaceutical Sciences*, 66(3):297–304.

[15] J. Takacs. "fourier amplitudok meghatarozasa operatorszamitassal". *Magyar Hiradastechnika (in Hungarian)*, 1953.

8 Appendix

Figure A: Flowchart scheme showing computational steps from 3.3-3.5.2:

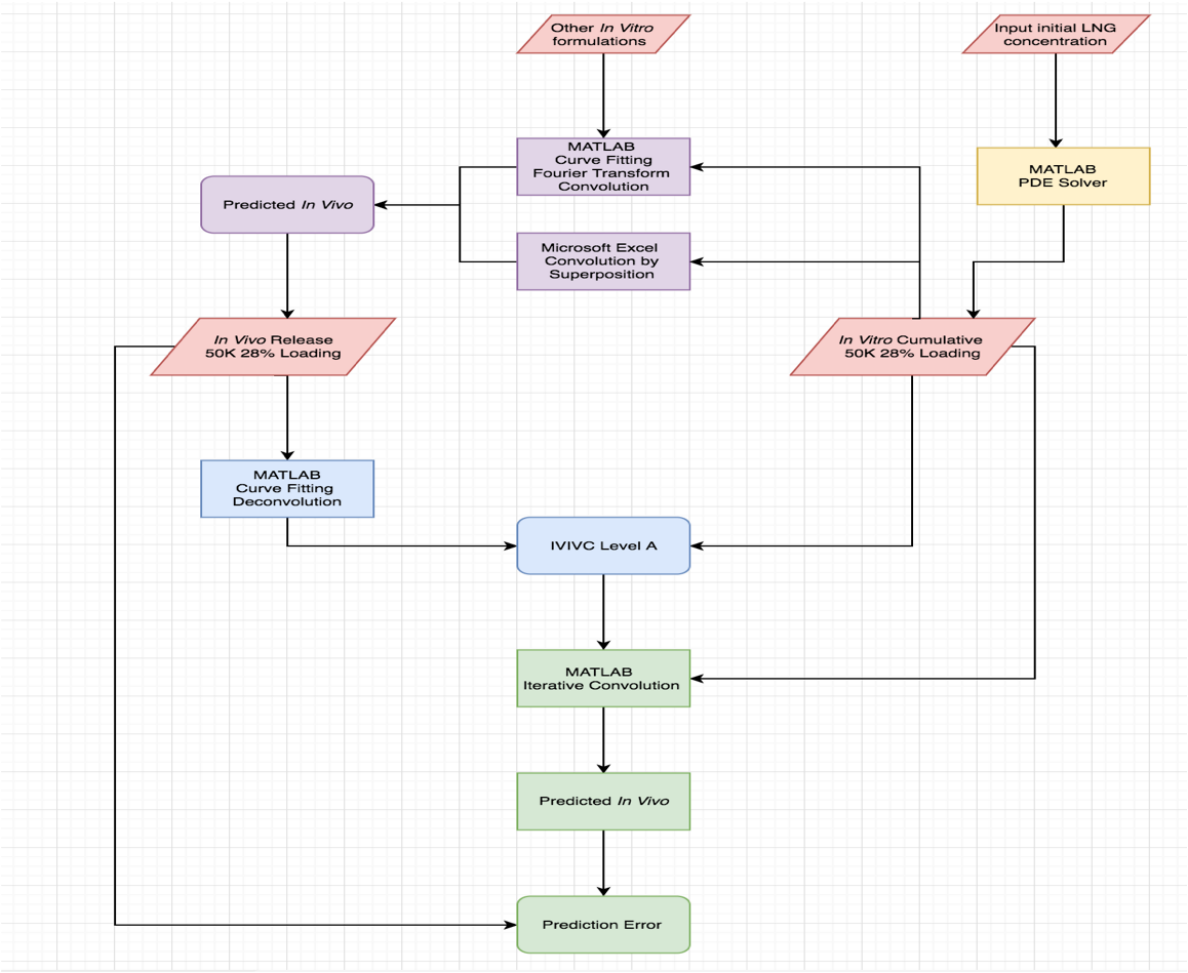

Red: Initial Data

Green: IVIVC Validation

Yellow: PDE Solver

Blue: IVIVC

Purple: Computational Predictions

Figure B: scheme showing computational steps within 3.5.2[5]

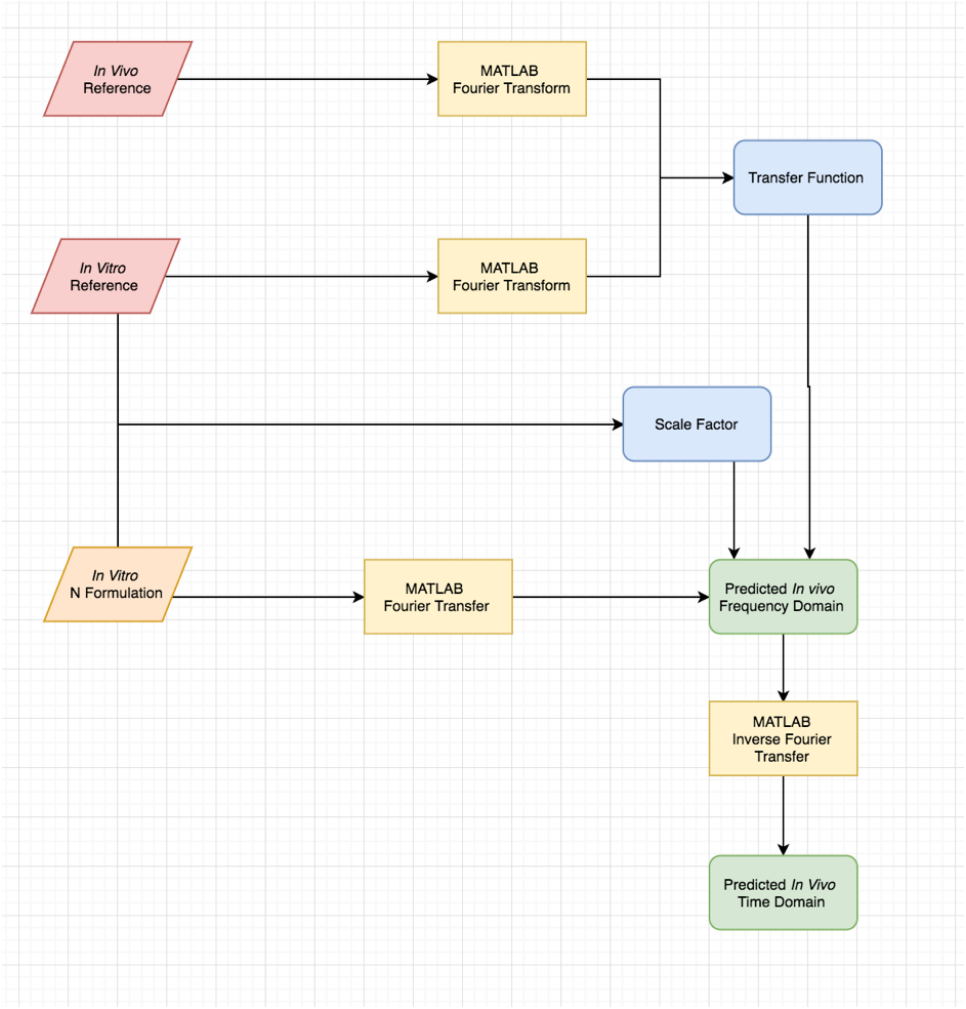

Red: Reference Data

Orange: Formulation Data

Yellow: MATLAB Fourier operations

Blue: Components of Prediction calculation

Green: Predicted Results